Neural Computation, Vol. 12 No. 10, pp. 2331-2353

Clustering Irregular Shapes Using High-Order Neurons

H. Lipson[1], H. T. Siegelmann[2]

[1]Mechnical Engineering Department
[2]Industrial Engineering and Management Department
Technion - Israel Institute of Technology, Haifa 32000, Israel
Current E-mail: [1]hlipson@mit.edu [2]iehava@ie.technion.ac.il

Abstract: This paper introduces a method for clustering irregularly shaped data arrangements using high-order neurons. Complex analytical shapes are modeled by replacing the classic synaptic weight of the neuron by high-order tensors in homogeneous coordinates. In the first and second order cases, this neuron corresponds to the classic neuron and ellipsoidal-metric neuron. We show how high order shapes can be formulated to follow the maximum-correlation activation principle and permit simple local Hebbian learning. We also demonstrate decomposition of spatial arrangements of data clusters including very close and partially overlapping clusters which are difficult to distinguish using classic neurons. Superior results are obtained for the IRIS data.

1 Introduction

In classical self-organizing networks, each neuron j is assigned a synaptic weight denoted by the column-vector $\boldsymbol{w}^{(j)}$. The winning neuron $j(\boldsymbol{x})$ in response to an input $\boldsymbol{x}$ is the one showing the highest *correlation* with the input, i.e. neuron j for which $\boldsymbol{w}^{(j)T}\boldsymbol{x}$ is the largest,

$$j(\mathbf{x}) = \arg_j \max \left\| \mathbf{w}^{(j)T}\mathbf{x} \right\| \qquad \text{Eq. 1}$$

where the operator $\|\cdot\|$ represents the Euclidean norm of a vector. The use of the term $\boldsymbol{w}^{(j)T}\boldsymbol{x}$ as the *matching criterion* corresponds to selection of the neuron exhibiting the maximum correlation with the input. Note that when the synaptic weights $\boldsymbol{w}^{(j)}$ are normalized to a constant Euclidean length, then the above criterion becomes the minimum Euclidean distance matching criterion

$$j(\mathbf{x}) = \arg_j \min \left\| \mathbf{x} - \mathbf{w}^{(j)} \right\|, \quad j = 1,2,\ldots,N \qquad \text{Eq. 2}$$

However, the use of a minimum-distance matching-criterion incorporates several difficulties. The minimum distance criterion implies that the features of the input domain are spherical, i.e., matching deviations are considered equally in all directions, and distances between features must be larger than the distances between points within a feature. These aspects preclude the ability to detect higher order, complex or ill-posed feature configurations and topologies, as these are based on higher geometrical properties such as *directionality* and *curvature.* This constitutes a major difficulty, especially when the input is of high dimensionality where such configurations are difficult to visualize and detect.

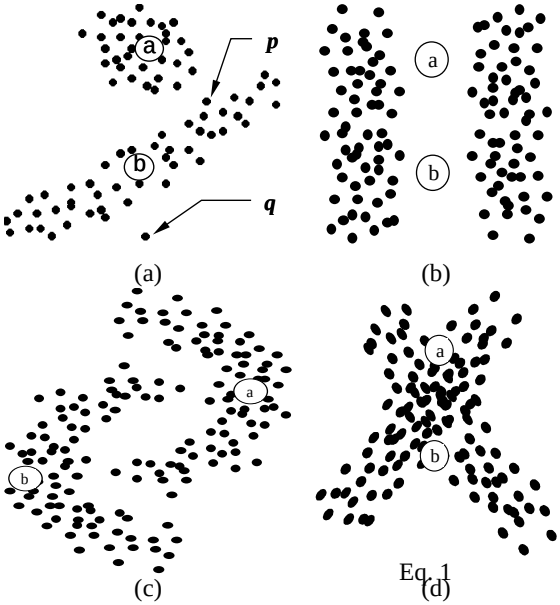

Figure 1. (a) Two data clusters with non-isotropic distributions, (b) close clusters, (c) curved clusters not linearly separable, (d) overlapping clusters

Consider, for example, the simple arrangements of two data clusters residing in a two dimensional domain, shown in Figure 1. The input data points are marked as small circles, and two classical neurons, **a** and **b**, are located at the centers of each cluster. In Figure 1(a), data cluster **b** exhibits a non-isotropic distribution; therefore, the nearest neighbor or maximum correlation criterion does not yield the desired classification because deviations cannot be considered equally in all directions. For example,

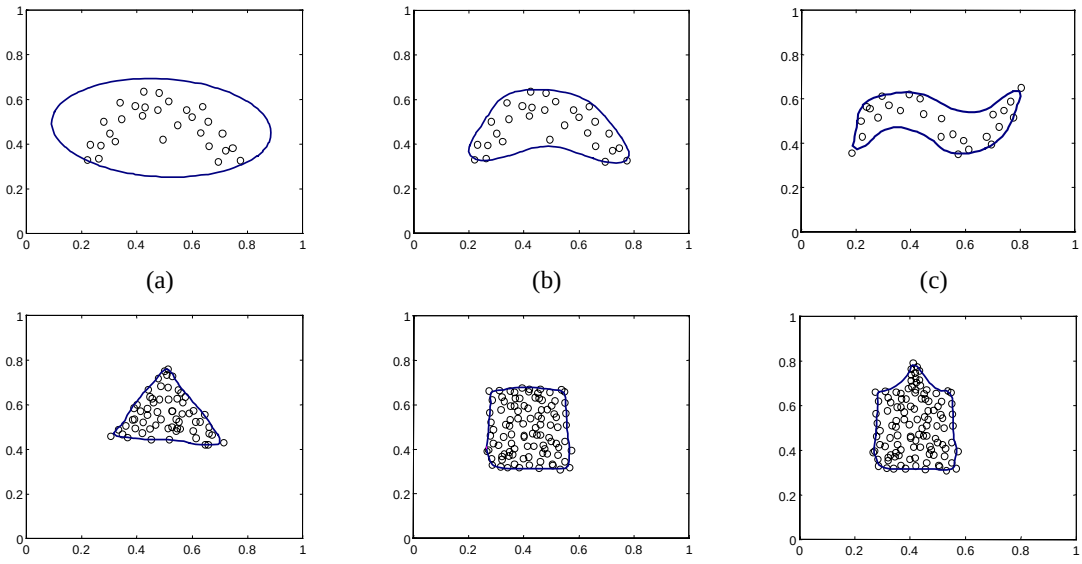

Figure 2. Some examples of single neuron shapes computed for the given clusters (after one epoch): (a)-(f) orders two to seven, respectively.

point *p* is farther away from neuron **b** than is point *q*, yet point *p* definitely belongs to cluster **b** while point *q* does not. Moreover, point *p* is closer to neuron **a** but clearly belongs to cluster **b**. Similarly, two close and elongated clusters will result in the neural locations shown in Figure 1(b). More complex clusters as shown in Figure 1(c) and Figure 1(d) may require still more complex metrics for separation.

There have been several attempts to overcome the above difficulties using second order metrics, namely ellipses and second order curves. Generally, the use of an inverse covariance matrix in the clustering metric enables capturing linear directionality properties of the cluster, and has been used in a variety of clustering algorithms. Gustafson and Kessel (1979) use the covariance matrix to capture ellipsoidal properties of clusters. Dave (1989) used fuzzy clustering with a non-Euclidean metric to detect lines in images. This concept was later expanded, and Krishnapuram *et al* (1995) use general second-order shells such as ellipsoidal shells and surfaces. For an overview and comparison of these methods see Frigui and Krishnapuram (1996). Abe and Thawonmas (1997) discuss a fuzzy classifier (ML) with ellipsoidal units. Incorporation of Mahalanobis (elliptical) metrics in neural networks was addressed by Kavuri and Venkatasubramanian (1993) for fault analysis applications and by Mao and Jain (1996) as a general competitive network with embedded principal component analysis units. Kohonen (1997) also discusses the use of adaptive tensorial weights to capture significant variances in the components of input signals, thereby introducing a weighted elliptic Euclidean distance in the matching law.

At the other end of the spectrum, non-parametric clustering methods such as agglomerative techniques (Blatt *et al*, 1996) avoid the need to provide a parametric shape for clusters, thereby permitting them to take arbitrary forms. However, agglomerative clustering techniques cannot handle overlapping clusters as shown in Figure 1(d). Overlapping clusters are common in real-life data and represent inherent uncertainty or ambiguity in the natural classification of the data. Areas of overlap are therefore of interest and should be explicitly detected.

This work presents an attempt to generalize the spherical/ellipsoidal scheme to more general metrics, thereby giving rise to a continuum of possible cluster shapes between the classic spherical/ellipsoidal units and the fully non-parametric approach. To visualize cluster metric, we draw a hypersurface at an arbitrary constant threshold of the metric. The shape of the resulting surface is characteristic of the shape of local dominance zone of the neuron, and will be referred to as the *shape* of the neuron. Some examples of neuron distance metrics yielding practically arbitrary shapes at various orders of complexity are shown in **Error! Reference source not found.** below. The shown hyper-surfaces are the optimal (tight) boundary of each cluster, respectively.

In general, the shape restriction of classic neurons is relaxed by replacing the weight vector or covariance matrix of a classic neuron with a general high-order tensor, which can capture multilinear correlations among the signals associated with the neurons. This permits also capturing shapes with holes and/or detached areas, as in Figure 3. We also use the concept of homogeneous coordinates to combine correlations of different orders into a single tensor.

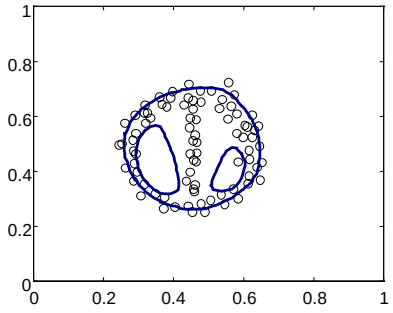

(a)

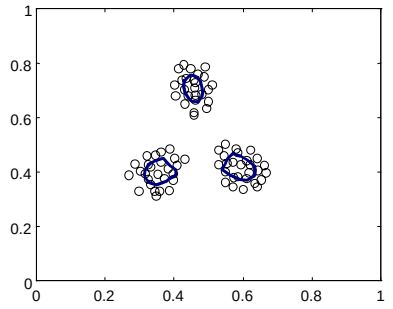

(b)

Figure 3. A shape neuron can have non-simple topology: (a) A single 5th order neuron with non-compact shape, including two "holes", (b) A single 4th order neuron with three detached active zones.

Although carrying the same name, our notion of high order neurons is different than the one used, for example, by Busch *et al* (1988), Giles *et al* (1988), Pollack (1991), Goudreau *et al* (1994) and Balestrino and Verona (1994). There, high order neurons are those that receive multiplied combinations of inputs rather than individual inputs. Those neurons were also not used for clustering or in the framework of competitive learning. It appears that high order neurons were generally abandoned mainly due to the difficulty in training such neurons and their inherent instability due to the fact that small variations in weight may cause a large variation in the output. Some also questioned the usefulness of high order statistics for improving predictions (Myung *et al*, 1992). In this paper we demonstrate a different notion of high-order neurons where the neurons are tensors, and their order pertains to their internal tensorial order rather than to the degree of the inputs. Our high order neurons exhibit good stability and excellent training performance with simple Hebbian learning. Furthermore, we believe that capturing high order information within a single neuron facilitates explicit manipulation and extraction of this information. We are not aware of work on general high order neurons being used for clustering or competitive learning in this manner.

This paper is organized as follows. Section 2 derives the tensorial formulation of a single neuron, starting with a simple second-order (elliptical) metric, moving into homogeneous coordinates and then increasing order for a general shape. Section 3 discusses the learning capacity of such neurons and their functionality within a layer. Finally, section 4 demonstrates an implementation of the proposed neurons on synthetic and real data. The paper concludes with some remarks on possible future extensions.

2 A "*general shape*" neuron

In the following sections we adopt the notation below:

$\boldsymbol{x}$, $\boldsymbol{w}$	column vectors
$\boldsymbol{W}$, $\boldsymbol{D}$	matrices
$\boldsymbol{x}^{(j)}$, $\boldsymbol{D}^{(j)}$	the j^{th} vector/matrix corresponding to the j^{th} neuron/class.
x_i, $\boldsymbol{D}_{ij}$	element of a vector/matrix
$\boldsymbol{x}_H$, $\boldsymbol{D}_H$	vector/matrix in homogeneous coordinates
m	order of the high-order neuron
d	the dimensionality of the input
N	the size of the layer (the number of neurons)
n	the number of inputs

The modeling constraints imposed by the maximum correlation matching criterion stem from the fact that the neuron's synaptic weight $\boldsymbol{w}^{(j)}$ has the same dimensionality as the input $\boldsymbol{x}$, i.e., the same dimensionality as a *single* point in the input domain, while in fact the neuron is modeling a *cluster* of points which may have higher order attributes such as directionality and curvature. We shall therefore refer to the classic neuron as a 'first-order' (zero degree) neuron, due to its correspondence to a *point* in multidimensional space.

To circumvent this restriction, we augment the neuron with the capacity to map additional geometric and topological information, by increasing its order. For example, as the first-order is a point neuron, the

second-order case will correspond to orientation and size components, effectively attaching a local oriented coordinate system with non-uniform scaling to the neuron center and using it to define a new distance metric. Thus each high-order neuron will represent not only the mean value of the data points in the cluster it is associated with, but also the principal directions, curvatures, etc. of the cluster and the variance of the data points along these directions. Intuitively, we can say that rather than defining a sphere, the high-order distance metric now defines a multi-dimensional oriented shape with an adaptive shape and topology (see **Error! Reference source not found.** and Figure 3).

In the following pages, we briefly review the ellipsoidal metric and established the basic concepts of encapsulation and base functions to be used in higher order cases where tensorial notation becomes more difficult to follow.

For a second-order neuron, define the matrix $\boldsymbol{D}^{(j)} \in \Re^{dxd}$ to encapsulate the direction and size properties of a neuron, for each dimension of the input, where d is the number of dimensions. Each row i of $\boldsymbol{D}^{(j)}$ is a unit row vector $\boldsymbol{v}_i^T$ corresponding to a principal direction of the cluster, divided by the standard deviation of the cluster in that direction (the square root of the variance σ_i). The Euclidean metric can now be replaced by the neuron-dependent metric

$$dist(\mathbf{x}, j) = \left\| \mathbf{D}^{(j)} \left(\mathbf{x} - \mathbf{w}^{(j)} \right) \right\|, \quad \text{where}$$

$$\mathbf{D}^{(j)} = \begin{bmatrix} \frac{1}{\sqrt{\sigma_1}} & 0 & \cdots & 0 \\ 0 & \frac{1}{\sqrt{\sigma_2}} & & \vdots \\ \vdots & & \ddots & 0 \\ 0 & \cdots & 0 & \frac{1}{\sqrt{\sigma_d}} \end{bmatrix} \begin{bmatrix} \mathbf{v}_1^T \\ \mathbf{v}_2^T \\ \vdots \\ \mathbf{v}_d^T \end{bmatrix}$$

such that deviations are normalized with respect to the variance of the data in the direction of the deviation. The new matching criterion based on the new metric becomes

$$i(\mathbf{x}) = \arg_j \min \left\| dist(\mathbf{x})^{(j)} \right\|$$
$$= \arg_j \min \left\| \mathbf{D}^{(j)} \left(\mathbf{x} - \mathbf{w}^{(j)} \right) \right\|, j = 1,2,\ldots,N$$

The neuron is now represented by the pair $(\boldsymbol{D}^{(j)}, \boldsymbol{w}^{(j)})$, where $\boldsymbol{D}^{(j)}$ represents rotation and scaling, and $\boldsymbol{w}^{(j)}$ represents translation. The values of $\boldsymbol{D}^{(j)}$ can be obtained from an eigenstructure analysis of the correlation matrix $\boldsymbol{R}^{(j)} = E\langle \boldsymbol{x}^{(j)}, \boldsymbol{x}^{(j)T} \rangle \in \Re^{dxd}$ of the data associated with neuron j. Two well known properties are derived from the eigenstructure of principal component analysis: (a) the eigenvectors of a correlation matrix $\boldsymbol{R}$ pertaining to the zero mean data vector $\boldsymbol{x}$ define the unit vectors $\boldsymbol{v}_i$ representing the principal directions along which the variances attain their extremal values, and (b) the associated eigenvalues define the extremal values of the variances σ_i. Hence

$$\mathbf{D}^{(j)} = \lambda^{(j)^{-\frac{1}{2}}} \mathbf{V}^{(j)},$$

where $\boldsymbol{\lambda}^{(j)} = diag(\boldsymbol{R}^{(j)})$ produces the eigenvalues of $\boldsymbol{R}^{(j)}$ in a diagonal form, and where $\mathbf{V}^{(j)} = eig(\boldsymbol{R}^{(j)})$ produces the unit eigenvectors of $\boldsymbol{R}^{(j)}$ in matrix form. Also, by definition of eigenvalue analysis of a general matrix $\boldsymbol{A}$,

$$\mathbf{AV} = \lambda \mathbf{V}$$

and hence

$$\mathbf{A} = \mathbf{V}^T \lambda \mathbf{V},$$

Now, since a term $\|\boldsymbol{a}\|$ equals $\boldsymbol{a}^T\boldsymbol{a}$, we can expand the term $\|\boldsymbol{D}^{(j)}(\boldsymbol{x}-\boldsymbol{w}^{(j)})\|$ of Eq. 4 as follows

$$\left\| \mathbf{D}^{(j)} \left(\mathbf{x} - \mathbf{w}^{(j)} \right) \right\|$$
$$= \left(\mathbf{x} - \mathbf{w}^{(j)} \right)^T \mathbf{D}^{(j)^T} \mathbf{D}^{(j)} \left(\mathbf{x} - \mathbf{w}^{(j)} \right),$$

Substituting Eq. 2 and Eq. 5, we see that

$$\mathbf{D}^{(j)^T} \mathbf{D}^{(j)} = \begin{bmatrix} \mathbf{v}_1, \mathbf{v}_2, \cdots, \mathbf{v}_d \end{bmatrix} \begin{bmatrix} \frac{1}{\sigma_1} & 0 & \cdots & 0 \\ 0 & \frac{1}{\sigma_2} & & \vdots \\ \vdots & & \ddots & 0 \\ 0 & \cdots & 0 & \frac{1}{\sigma_d} \end{bmatrix} \begin{bmatrix} \mathbf{v}_1^T \\ \mathbf{v}_2^T \\ \vdots \\ \mathbf{v}_d^T \end{bmatrix} \quad \text{Eq. 3}$$

$$= \mathbf{R}^{(j)^{-1}}$$

meaning that the scaling and rotation matrix is, in fact, the inverse of $\boldsymbol{R}^{(j)}$. Hence,

$$i(\mathbf{x}) = \arg_j \min \left[\left(\mathbf{x} - \mathbf{w}^{(j)} \right)^T \mathbf{R}^{-1} \left(\mathbf{x} - \mathbf{w}^{(j)} \right) \right], \quad \text{Eq. 4}$$
$$j = 1,2,\ldots,N$$

which corresponds to the term used by Gustafson and Kessel, (1979) and in the maximum likelihood Gaussian classifier (Duda and Hart, 1973).

Eq. 9 involves two explicit terms, $\boldsymbol{R}^{(j)}$ and $\boldsymbol{w}^{(j)}$, representing of the orientation and size information, respectively. Implementations involving ellipsoidal metrics therefore need to track these two quantities separately, in a two-stage step. Separate tracking, however, cannot be easily extended to higher orders,

which requires simultaneous tracking of additional higher order qualities such as curvatures. We therefore use an equivalent representation that 'encapsulates' these terms into one, and permits a more systematic extension to higher orders.

We combine these two coefficients into one *expanded covariance* denoted $\boldsymbol{R}_{\mathrm{H}}^{(\mathrm{j})}$ in homogenous coordinates (Faux and Pratt, 1981), as

$$\mathbf{R}_H^{(j)} = \frac{1}{n} \quad \mathbf{x}_H^{(j)} \mathbf{x}_H^{(j)^T} = E\left\langle \mathbf{x}_H^{(j)}, \mathbf{x}_H^{(j)^T} \right\rangle$$

where in homogenous coordinates $\boldsymbol{x}_{\mathrm{H}}^{(\mathrm{j})} \in \Re^{(d+1)\times 1}$ and is defined by $\mathbf{x}_H = \begin{bmatrix} \mathbf{x} \\ \cdots \\ 1 \end{bmatrix}$.

In this notation, the expanded covariance contains also coordinate permutations involving "1" as one of the multiplicands and so different (lower) orders are introduced. Consequently, $\boldsymbol{R}_{\mathrm{H}}^{(\mathrm{j})} \in \Re^{(d+1)\times(d+1)}$. In analogy to the 'correlation matrix memory' and 'autoassociative memory' (Haykin, 1994), the extended matrix $\boldsymbol{R}_{\mathrm{H}}^{(\mathrm{j})}$, in its general form, can be viewed as '*homogeneous autoassociative tensor*'. Now the new matching criterion becomes simply

$$\begin{aligned} i(\mathbf{x}) &= \arg_j \min\left[\mathbf{X}^T \mathbf{R}_H^{(j)^{-1}} \mathbf{X}\right] \\ &= \arg_j \min\left\| \mathbf{R}_H^{(j)^{-\frac{1}{2}}} \mathbf{X} \right\|, \\ &= \arg_j \min\left\| \mathbf{R}_H^{(j)^{-1}} \mathbf{X} \right\|, \quad j = 1,2,\ldots,N \end{aligned}$$

This representation retains the notion of maximum correlation, and for convenience, we now denote $\boldsymbol{R}_{\mathrm{H}}^{-1(\mathrm{j})}$ as the *synaptic tensor*.

When we moved into homogenous coordinates, we gained the following:

1. The eigenvectors of the original covariance matrix $\boldsymbol{R}^{(\mathrm{j})}$ represented directions. The eigenvectors of the homogeneous covariance matrix $\boldsymbol{R}_{\mathrm{H}}^{(\mathrm{j})}$ corresponds to the both the principal directions *and* the offset (i.e. both second-order and first-order) properties of the cluster accumulated in $\boldsymbol{R}_{\mathrm{H}}^{(\mathrm{j})}$. In fact, the elements of each eigenvector correspond to the coefficient of the line equation $ax+by+\ldots+c=0$. This property permits direct extension to higher order tensors in the next section, where direct eigenstructure analysis is not well defined.

2. The transition into homogeneous coordinates dispensed with the problem created by the fact that the eigenstructure properties cited above pertained only to zero-mean data, whereas $\boldsymbol{R}_{\mathrm{H}}^{(\mathrm{j})}$ is defined as the covariance matrix of *non*-zero-mean data. By using homogeneous coordinates, we effectively consider the translational element of the cluster as yet another (additional) dimensions. In this higher space, the data can be considered to be zero-mean.

2. 1 Higher orders

Eq. 10

The ellipsoidal neuron can capture only linear directionality, but not curved directionalities such as that appearing, for instance, in a *fork*, in a curved or in a sharp-cornered shape. In order to capture more complex spatial configurations, higher order geometries must be introduced.

The classic neuron possesses a synaptic weight vector $\boldsymbol{w}^{(\mathrm{j})}$ which correspond to a *point* in the input domain. The synaptic weight $\boldsymbol{w}^{(\mathrm{j})}$ can be seen as the first order average of its signals, i.e., $\boldsymbol{w}^{(\mathrm{j})}=\Sigma\boldsymbol{x}_{\mathrm{H}}$ (the last element $\boldsymbol{x}_{\mathrm{H}d+1}=1$ of the homogeneous coordinates has no effect in this case). Ellipsoidal units hold information regarding the linear correlations among the coordinates of data points represented by the neuron, by using $\boldsymbol{R}_{\mathrm{H}}^{(\mathrm{j})}=\Sigma\boldsymbol{x}_{\mathrm{H}}\boldsymbol{x}_{\mathrm{H}}^{\mathrm{T}}$. Each element of $\boldsymbol{R}_{\mathrm{H}}$ is thus a proportionality *constant* relating two specific dimensions of the cluster. The second-order neuron can therefore be regarded as a second-order approximation of the corresponding data distribution. Eq. 11
Higher order relationships can be introduced by considering correlations among more than just two variables. We may consequently introduce a neuron capable of modeling a *d-dimensional* data cluster to an m^{th}*-order* approximation.

Higher order correlations are obtained by multiplying the generating vector $\boldsymbol{x}_{\mathrm{H}}$ by itself, in successive outer products, more than just once. The process yields a *covariance tensor*, rather than just a *covariance matrix* (which is a second-order tensor). The resulting homogeneous covariance tensor is thus represented by a *2(m-1)*-order tensor of rank *d+1*, denoted by $\boldsymbol{Z}_{\mathrm{H}}^{(\mathrm{j})} \in \Re^{(d+1)\times\ldots\times(d+1)}$, obtained by *2(m-1)* outer products of $\boldsymbol{x}_{\mathrm{H}}$ by itself:

$$\mathbf{Z}_H^{(j)} = \mathbf{x}_H^{2(m-1)}$$

The exponent consists of the factor *(m-1)*, which is the degree of the approximation, and a factor of 2 since we are performing *auto*-correlation so the function is multiplied by itself. In analogy to reasoning that lead to Eq. 11, each eigenvector (now an eigen*tensor* of order *m-1)* corresponds to the coefficients of a principal curve, and multiplying it by an input points produces an approximation of the distance of that

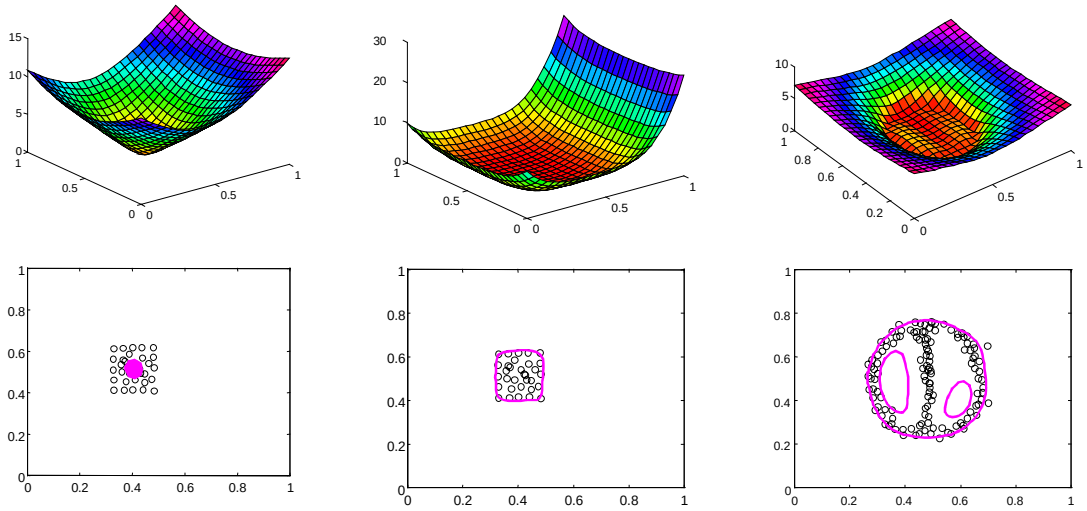

(a) (b) (c)

Figure 4. Metrics of various orders: (a) a regular neuron (spherical metric), (b) a 'square' neuron, (c) a neuron with 'two holes'

input point from the curve. Consequently, the inverse of the tensor $\mathbf{Z}_H^{(j)}$ can then be used to compute the high-order correlation of the signal with the nonlinear shape neuron, by simple tensor multiplication:

$$i(\mathbf{x}) = \arg_j \min \left\| \mathbf{Z}_H^{(j)^{-1}} \otimes x_H^{m-1} \right\|, \quad j = 1,2,\ldots,N$$

where $\otimes$ denotes tensor multiplication. Note that the covariance tensor can only be inverted if its order is an even number, as satisfied by Eq. 12. Note also that amplitude operator is carried out by computing the root of the sum of the squares of the elements of the argument. The computed metric is now not necessarily spherical and may take various other forms as plotted in **Error! Reference source not found.**.

In practice however, high-order tensor inversion is not directly required. To make this analysis simpler, we use a Kronecker notation for tensor products (see Graham, 1981). Kronecker tensor product 'flattens out' the elements of $X \otimes Y$ into a large matrix formed by taking all possible products between the elements of X and those of Y. For example, if X is a 2 by 3 matrix, then $X \otimes Y$ is

$$X \otimes Y = \left[\begin{array}{c|c|c} Y \cdot X_{1,1} & Y \cdot X_{1,2} & Y \cdot X_{1,3} \\ \hline Y \cdot X_{2,1} & Y \cdot X_{2,2} & Y \cdot X_{2,3} \end{array}\right]$$

where each block is a matrix of the size of Y. In this notation, the internal structure of higher-order tensors is easier to perceive and their correspondence to linear regression of principal polynomial curves is revealed. Consider, for example, a fourth order covariance tensor of the vector $\boldsymbol{x}=\{x,y\}$. The fourth-order tensor corresponds to the simplest non-linear neuron according to Eq. 12, and takes the form of the 2×2×2×2 tensor

$$E\langle \mathbf{x}\otimes\mathbf{x}\otimes\mathbf{x}\otimes\mathbf{x}\rangle = E\langle \mathbf{R}\otimes\mathbf{R}\rangle \qquad \text{Eq. 13}$$

$$= \frac{1}{n} \begin{bmatrix} x^2 & xy \\ xy & y^2 \end{bmatrix} \otimes \begin{bmatrix} x^2 & xy \\ xy & y^2 \end{bmatrix} \qquad \text{Eq. 15}$$

$$= \frac{1}{n} \left[\begin{array}{cc|cc} x^4 & x^3y & x^3y & x^2y^2 \\ x^3y & x^2y^2 & x^2y^2 & xy^3 \\ \hline x^3y & x^2y^2 & x^2y^2 & xy^3 \\ x^2y^2 & xy^3 & xy^3 & y^4 \end{array}\right]$$

The homogeneous version of this tensor includes also all lower-order permutations of the coordinates of $\boldsymbol{x}_H=\{x,y,1\}$, namely, the 3×3×3×3 tensor

$$\mathbf{Z}_{H(4)} = E\langle \mathbf{x}_H, \mathbf{x}_H, \mathbf{x}_H, \mathbf{x}_H \rangle = E\langle \mathbf{R}_H, \mathbf{R}_H \rangle$$

$$= \frac{1}{n} \begin{bmatrix} x^2 & xy & x \\ xy & y^2 & y \\ x & y & 1 \end{bmatrix} \otimes \begin{bmatrix} x^2 & xy & x \\ xy & y^2 & y \\ x & y & 1 \end{bmatrix} = \qquad \text{Eq. 14}$$

$$\frac{1}{n}\begin{bmatrix} x^4 & x^3y & x^3 & x^3y & x^2y^2 & x^2y & x^3 & x^2y & x^2 \\ x^3y & x^2y^2 & x^2y & x^2y^2 & xy^3 & xy^2 & x^2y & xy^2 & xy \\ x^3 & x^2y & x^2 & x^2y & xy^2 & xy & x^2 & xy & x \\ x^3y & x^2y^2 & x^2y & x^2y^2 & xy^3 & xy^2 & x^2y & xy^2 & xy \\ x^2y^2 & xy^3 & xy^2 & xy^3 & y^4 & y^3 & xy^2 & y^3 & y^2 \\ x^2y & xy^2 & xy & xy^2 & y^3 & y^2 & xy & y^2 & y \\ x^3 & x^2y & x^2 & x^2y & xy^2 & xy & x^2 & xy & x \\ x^2y & xy^2 & xy & xy^2 & y^3 & y^2 & xy & y^2 & y \\ x^2 & xy & x & xy & y^2 & y & x & y & 1 \end{bmatrix}$$

Remark. It is immediately apparent that the above matrix corresponds to the matrix to be solved for finding a least squares fit of a conic section equation $ax^2+by^2+cxy+dx+ey+f=0$ to the data points. Moreover, the set of eigenvectors of this matrix corresponds to the coefficients of the set of mutually orthogonal best-fit conic section curves that are the principal curves of the data. This notion adheres with Gnanadesikan's method for finding principal curves (Gnanadesikan, 1977). Now, substitution of a data point into the equation of a principal curve yields an approximation of the distance of the point from that curve, and the sum of squared distances amounts to Eq. 13. Note that each time we increase complexity, we are seeking a set of principal curves of one degree higher. This implies that the least-squares matrix needs to be *two* degrees higher (because it is minimizing the *squared* error), thus yielding the coefficient *2* in the exponent of Equation 12.

3 Learning and functionality

In order to show that higher-order shapes are a direct extension of classic neurons, we show that they are also subject to simple Hebbian learning. Following an interpretation of Hebb's postulate of learning, synaptic modification (i.e., learning) occurs when there is a correlation between presynaptic and postsynaptic activities. We have already shown in Eq. 11 above that (a) the presynaptic activity $\boldsymbol{x}_H$ and postsynaptic activity of neuron *j* coincide when the synapse is strong, i.e. $\boldsymbol{R}_H^{(j)-1}\boldsymbol{x}_H$ is minimum. We now proceed to show that, in accordance with Hebb's postulate of learning, (b) it is sufficient to incur self-organization of the neurons by increasing synapse strength when there is a coincidence of presynaptic and postsynaptic signals.

In order to provide quality (b) above, we need to show how self organization is obtained merely by increasing $\boldsymbol{R}_H^{(j)}$, where *j* is the winning neuron. As each new data point arrives at a specific neuron *j* in the net, the synaptic weight of that neuron is adapted by the incremental corresponding to Hebbian learning,

$$\mathbf{Z}_H^{(j)}(k+1) = \mathbf{Z}_H^{(j)}(k) + \eta(k)\mathbf{x}_H^{(j)2(m-1)} \quad \text{Eq. 16}$$

where *k* is the iteration counter and $\eta(k)$ is the iteration-dependent learning rate coefficient. It should be noted that in Eq. 12, $\boldsymbol{Z}_H^{(j)}$ becomes a *weighted sum* of the input signals $\boldsymbol{x}_H^{2(m-1)}$ (unlike $\boldsymbol{R}_H$ in Eq. 10, which a *uniform sum*). The eigenstructure analysis of a weighted sum still provides the principal components under the assumption that the weights are uniformly distributed over the cluster signals. This assumption holds true if the process generating the signals of the cluster is stable over time - a basic assumption of all neural network algorithms (Bishop, 1997). In practice this assumption is easily acceptable, as will be demonstrated in the following sections.

In principle, continuous updating of the covariance tensor may create instability in a competitive environment, as a winner neuron becomes more and more dominant. To force competition, the covariance tensor can be normalized using any of a number of factors dependent on the application, such as the number of signals assigned to the neuron so far, or the distribution of data among the neuron (forcing uniformity). However, a more 'natural' factor for normalization is the size/complexity of the neuron.

A second order neuron is geometrically equivalent to a *d*-dimensional hyper-ellipsoid. A neuron may be therefore normalized by a factor *V* proportional to the hyper-ellipsoids' *d*-volume. This volume is proportional to the standard deviations σ along each axis, namely

$$V \propto \sigma_1 \cdot \sigma_2 \cdot \ldots \cdot \sigma_d = \prod_{i=1}^{d} \sigma_i \propto \frac{1}{\det\left|\mathbf{R}^{(j)}\right|}$$

During the competition phase, the factors $\boldsymbol{R}^{(j)}\boldsymbol{x}/V$ are compared, rather than just $\boldsymbol{R}^{(j)}\boldsymbol{x}$, thus promoting smaller neurons and forcing neurons to become equally 'fat'. The final matching criteria for a homogeneous representation is therefore given by

$$j(\mathbf{x}) = \arg_j \min\left\|\hat{\mathbf{R}}_H^{-1(j)}\mathbf{x}_H\right\|, j = 1,2,\ldots,N,$$

where

$$\hat{\mathbf{R}}_H^{(j)} = \frac{\mathbf{R}_H^{(j)}}{\det\left|\mathbf{R}_{\mathbf{H}}^{(j)}\right|}$$

Covariance tensors of higher order neurons can also be normalized by its determinant. However, unlike second order neurons, higher-order shapes are not necessarily convex, and hence their volume is not

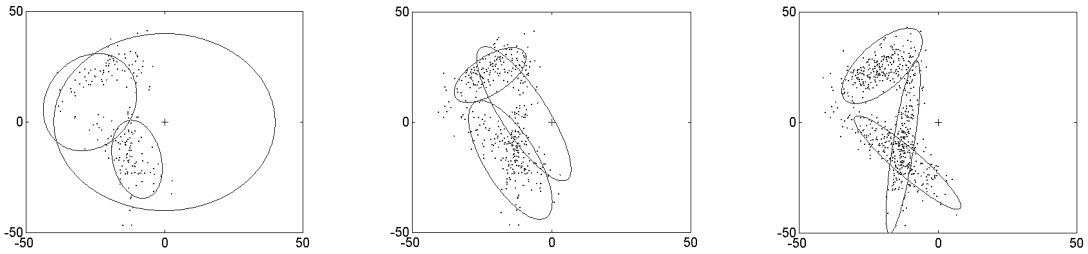

(a) (b) (c)

Figure 5 (a)-(c) Stages in self classification of overlapping clusters, after learning 200, 400, and 650 data points, respectively (one epoch).

necessarily proportional to their determinant. The determinant of higher order tensors therefore relates to a more complex characteristics, which include the deviation of the data points from the principal curves and the curvature of the boundary. Nevertheless, our experiments showed that this is a simple and effective means of normalization that promotes small and simple shapes over complex and/or large concave fittings to data. The relationship between geometric shape and the tensor determinant should be investigated further for more elaborate use of the determinant as a normalization criteria.

Finally, in order to determine the likelihood of a point being associated with a particular neuron, we need to assume a distribution function. Assuming Gaussian distribution, the likelihood $p^{(j)}(\mathbf{x}_H)$ of data point $\mathbf{x}_H$ being associated with cluster j is proportional to the distance from the neuron, and is given by

$$p^{(j)}(\mathbf{x}_H) = \frac{1}{(2\pi)^{d/2}} e^{-\frac{1}{2}\left\|\hat{\mathbf{z}}^{(j)}\mathbf{x}_H\right\|^2} \quad \text{Eq. 21}$$

4 Algorithm Summary

To conclude the previous sections, we provide a summary of the high-order competitive learning algorithm both for unsupervised and supervised learning. These are the algorithms that were used in the test cases described later in section 5.

4. 1 Unsupervised competitive learning

(1) ***Select layer size*** *(no. of neurons n) and neuron order (m) for given problem. Number of neurons can change over time.*

(2) ***Initialize all neurons*** *with $Z_H=1/n\ x_H^{2(m-1)}$ where sum is taken over all input data or a representative portion of it, or unit tensor or random numbers if no data is available. To compute this value, write down x_H^{m-1} as a vector with all m-th degree permutations of $\{x_1,x_2\ldots,x_d,1\}$, and compute Z_H as a matrix averaging the outer product of these vectors. Store Z_H and Z_H^{-1}/f, for each neuron, where f is a normalization factor (e.g. Eq. 20). Noise can be added.*

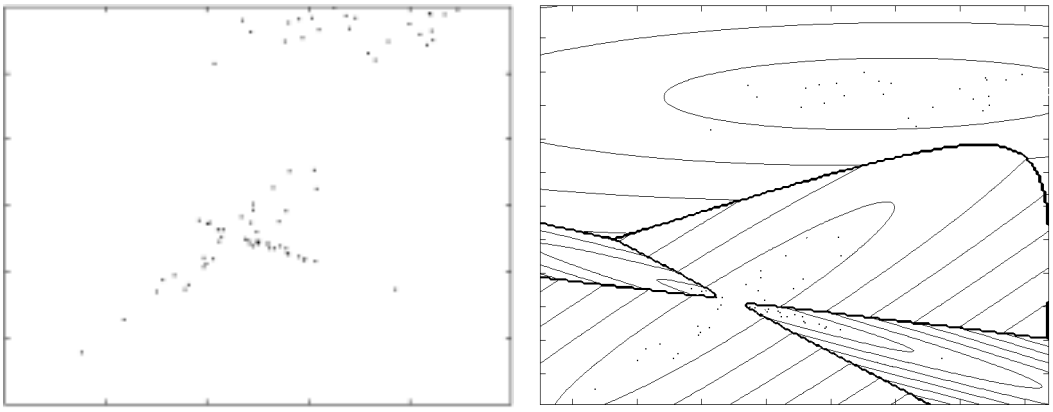

(a) (b)

Figure 6. (a) Original data set, (b) self-organized map of the data set; dark curves are the decision boundaries, light lines show the local distance metric within each cell. Note how the decision boundary in the overlap area accounts for the different distribution variances.

Method	Epochs	# misclassified or unclassified
Super Paramagnetic (Blatt *et al*, 1996)		25
LVQ / GLVQ (Pal *et al*, 1993)	200	17
K-Means (Mao and Jain, 1996)		16
HEC (Mao and Jain, 1996)		5
2nd-order Unsupervised	20	**4**
3rd-order Unsupervised	30	**3**

Table 1. Comparison of self-organization results[1] for IRIS data

(3) ***Compute winner*** *for input x as follows: first compute vector* x_H^{m-1} *from x as in section (2), and then multiply it by the stored matrix* Z_H^{-1}/f. *Winner neuron j is the one for which modulus of the product vector is smallest.*

(4) ***Output winner*** *j.*

(5) ***If in training phase, update winner*** *by adding* $x_H^{2(m-1)}$ *to* $Z_H^{(j)}$ *weighted by the learning coefficient* $\eta(k)$ *where k is the iteration counter . Store* Z_H *and* Z_H^{-1}/f, *for the updated neuron.*

(6) *Goto (3)*

4. 2 Supervised learning

(1) ***Set layer size*** *(no. of neurons) to number of classes and select neuron order (m) for given problem.*

(2) ***Train:*** *for each neuron, compute* $Z_H^{(j)}=1/n \; x_H^{2(m-1)}$ *where sum is taken over all training points to be associated with that neuron. To compute this value, write down* x_H^{m-1} *as a vector with all m-th degree permutations of* $\{x_1,x_2\ldots,x_d,1\}$, *and* Z_H *as a matrix summing the outer product of these vectors. Store* Z_H^{-1}/f *for each neuron where f is a normalization factor (e.g. Eq. 20).*

(3) ***Test:*** *Use test points to evaluate quality of training.*

(4) ***Use:*** *for each new input x: first compute vector* x_H^{m-1} *from x as in section (2), and then multiply it by the stored matrix* Z_H^{-1}/f. *Winner j is the one for which modulus of the product vector is smallest.*

5 Implementation with synthesized and real data

The proposed neuron can be used as an element in any network by replacing lower-dimensionality neurons, and will enhance the modeling capability of each neuron. Depending on the application of the net, this may lead to improvement or degradation of the overall performance of the layer, due to the added degrees of freedom. This section provides some examples of an implementation at different orders, in both supervised and unsupervised learning.

Order	Epochs	# misclassified	
		Average	Best
3-Hidden-Layer N.N. (Abe *et al*, 1997)	1000	2.2	1
Fuzzy Hyperbox (Abe *et al*, 1997)			2
Fuzzy Ellipsoids (Abe *et al*, 1997)	1000		1
2nd-order Supervised	1	3.08	1
3rd-order Supervised	1	2.27	1
4th-order Supervised	1	1.60	**0**
5th-order Supervised	1	**1.07**	**0**
6th-order Supervised	1	1.20	**0**
7th-order Supervised	1	1.30	**0**

Table 2. Supervised classification results for IRIS data. Our results after one training epoch, with 20% cross validation. Averaged results are for 250 experiments.

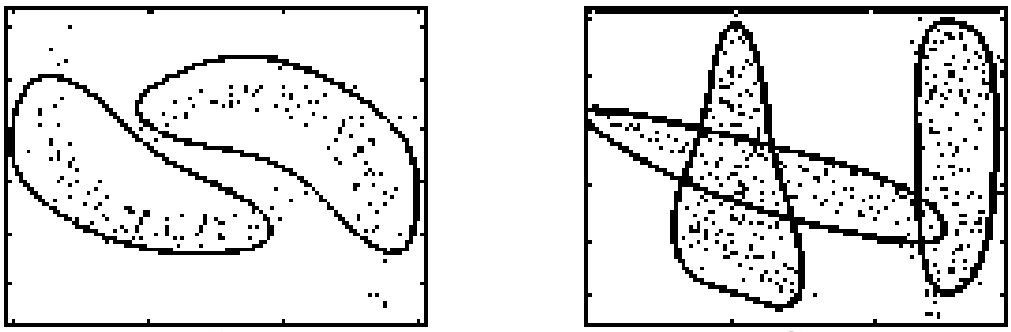

(a) (b)

Figure 7. Self-classification of synthetic point clusters using 3rd order neurons

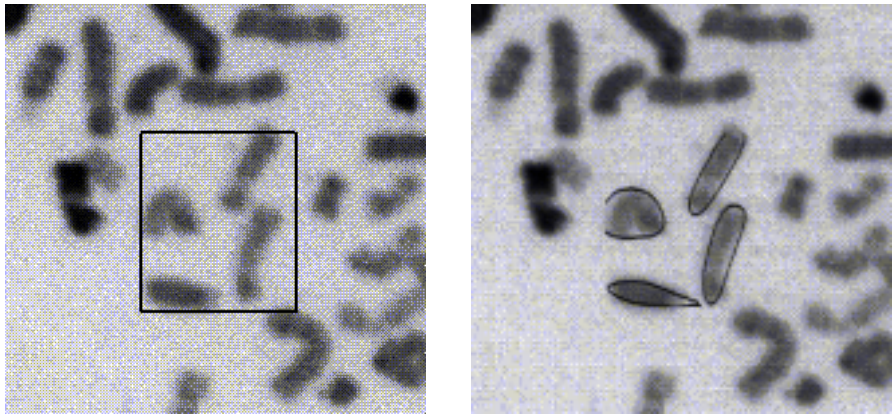

(a) (b)

Figure 8. Chromosome separation (a) Designated area (b) Four 3rd order neuron self organized to mark the chromosomes in designated area; data from Schrock (1996)

First, we discuss two examples of second order (ellipsoidal) neurons to show that our formulation is compatible with previous work on ellipsoidal neural units (e.g. Mao and Jain, 1996). **Error! Reference source not found.** illustrates how a competitive network consisting of three second-order neurons gradually evolves to model a two dimensional domain exhibiting three main activation areas with significant overlap. The second order neurons are visualized as ellipses with their boundaries drawn at 2σ of the distribution.

The next test uses a two-dimensional distribution of three arbitrary clusters, consisting of a total of 75 data points, shown in **Error! Reference source not found.**(a). The network of three 2nd order neurons self-organized to map this data set and creates the decision boundaries shown in **Error! Reference source not found.**(b). The dark curves are the decision boundaries, while the light lines show the local distance metric within each cell. Note how the decision boundary in the overlap area accounts for the different distribution variances.

The performance of the different orders of shape neuron has also been assessed on the IRIS Data (Anderson, 1939). Anderson's time-honored data set has become a popular benchmark problem for clustering algorithms. The data set consists of four quantities measured on each of 150 flowers chosen from three species of Iris: Iris Setosa, Iris Versicolor and Iris Virginica. The data set constitutes 150 points in four-dimensional space. Some results of other methods are compared in the **Error! Reference source not found.** below. It should be noted that the results presented in the table are 'best results'; 3rd order neurons are not always stable, i.e. the layer sometimes converges into different classifications[1].

[1] Performance of 3rd order neurons was evaluated with a layer consisting of three neurons randomly initialized with normal distribution within the input domain with mean and variance of the input, and with learning factor of 0.3 decreasing asymptotically towards zero. Of 100 experiments carried out, 95%

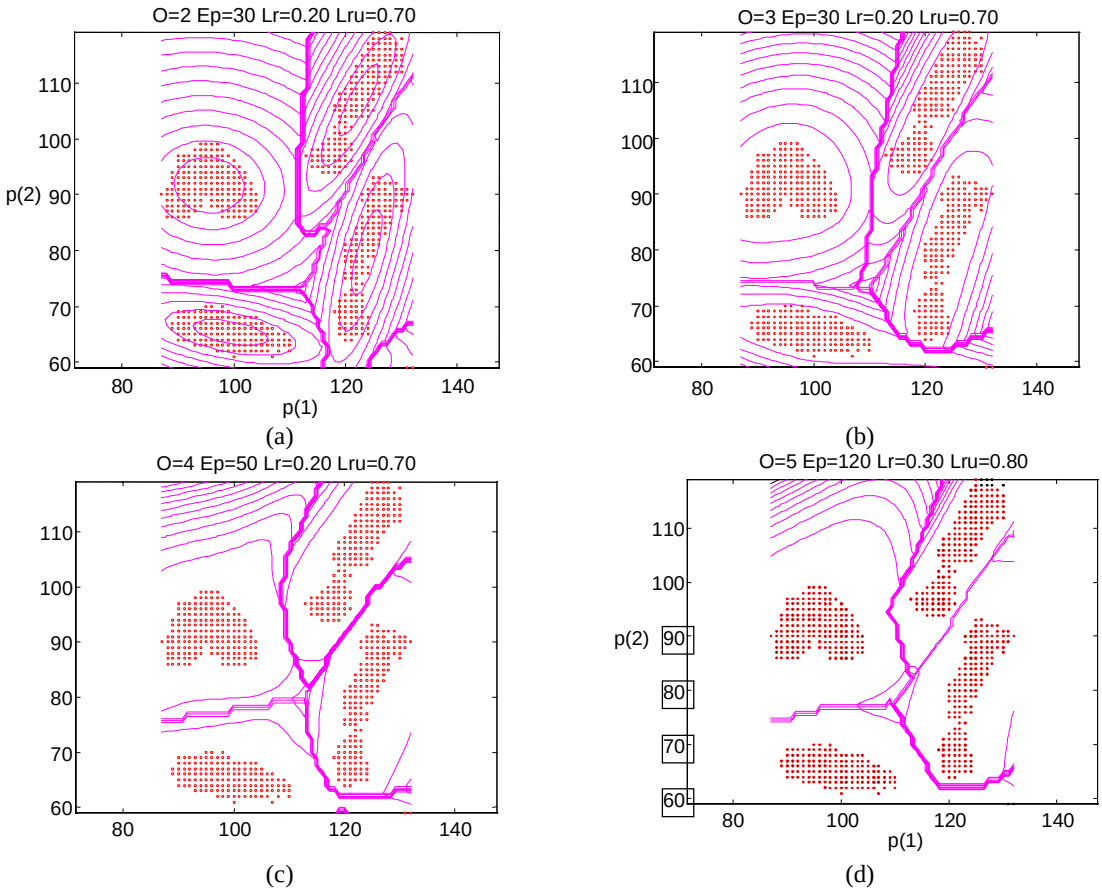

Figure 9. Self organization for chromosome separation (a)-(d) 2nd-5th order, respectively

The neurons have also been tried also in a supervised setup. In supervised mode, we use the same training setup of Eq. 10 and Eq. 12, but train each neuron individually on the signals associated with it, using the equation

$$\mathbf{Z}_H^{(j)} = \mathbf{x}_H^{2(m-1)}, \quad \mathbf{x}_H \in \Psi^{(j)} \qquad \text{Eq. 22}$$

where in homogenous coordinates $\mathbf{x}_H = \begin{bmatrix} \mathbf{x} \\ \cdots \\ 1 \end{bmatrix}$ and $\Psi^{(j)}$ is the *j*'th class.

In order to evaluate the performance of this technique, we trained each neuron on a random selection of 80% of the data points of its class, and then tested the classification of the whole data set (including the remaining 20% for cross validation). The test determined the most active neuron for each input and compared it with the manual classification. This test was repeated 250 times, with the average and best results shown in **Error! Reference source not found.**, along with results reported for other methods. It appears that on average, supervised learning for this task reaches an optimum with 5th order neurons.

Error! Reference source not found. shows classification results using 3rd order neurons for an arbitrary distribution containing close and overlapping clusters.

Finally, **Error! Reference source not found.** shows an application of 3rd-5th order neurons to detection and modeling of chromosomes in a human cell. The corresponding separation maps and convergence error rates are shown in **Error! Reference source not found.** and in **Error! Reference source not found.**, respectively.

---

locked correctly on the clusters, with average 7.6 (5%) misclassifications after 30 epochs. Statistics on performance of cited works have not been reported. Download MATLAB demos from *http://www.cs.brandeis.edu/~lipson/papers/geom.htm*

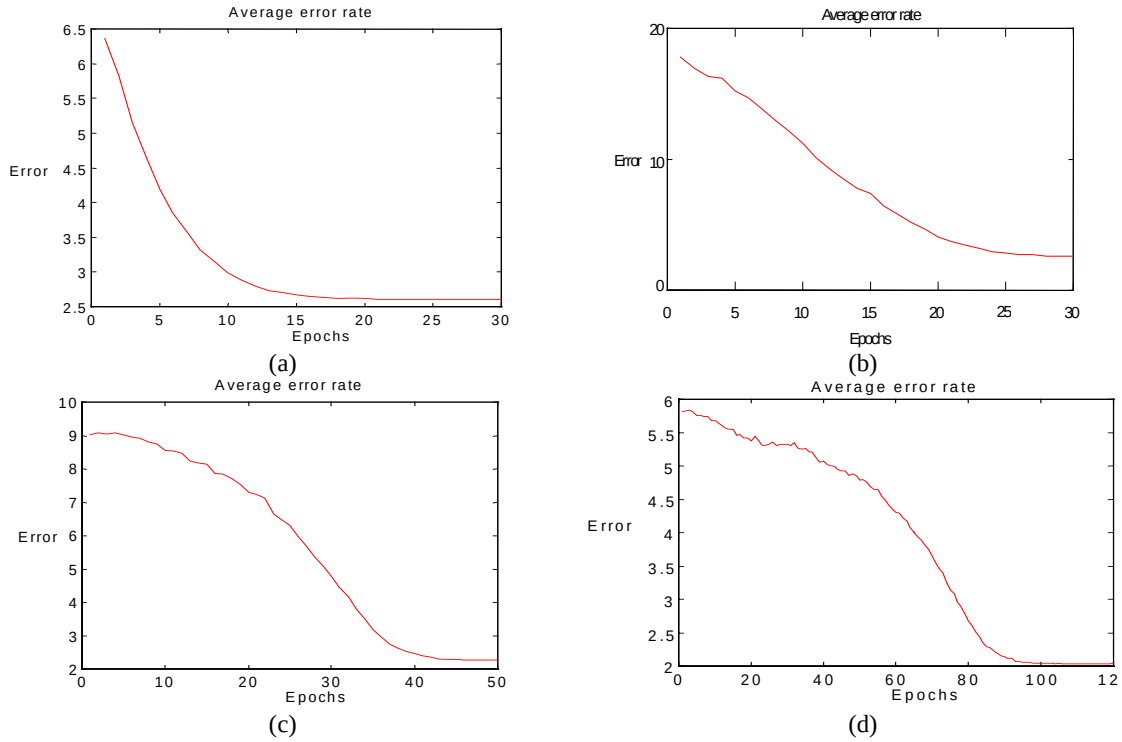

Figure 10. Average error rate in self-organization for chromosome separation of **Error! Reference source**

6 Conclusions and further research

In this paper, we have introduced high-order shape neurons and demonstrated their practical use for modeling the structure of spatial distributions and for geometric feature recognition. Although high-order neurons do not directly correspond to neurobiological details, we believe that they can provide powerful data modeling capabilities. In particular, they exhibit useful properties for correctly handling close and partially overlapping clusters. Furthermore, we have shown that ellipsoidal and tensorial clustering methods, as well as classic competitive neurons are special cases of the general-shape neuron. We showed how lower-order information can be 'encapsulated' using tensor representation in homogeneous coordinates, enabling systematic continuation to higher order metrics. This formulation also allows for direct extraction of the encapsulated high-order information in the form of principal curves, represented by the eigentensors of each neuron.

The use of shapes as neurons raises some further practical questions, which have not been addressed in this paper and require further research, and are listed below. Although most of these issues pertain to neural networks in general, the approach here may be different.

- **Number of neurons.** In the examples provided, we have explicitly used the number of neurons appropriate to the number of clusters. The question of network size is applicable to most neural architecture. However, our experiments showed that over specification tends to cause clusters to split into sub-sections, while under-specifications may cause clusters to unite.

- **Initial weights**. It is well known that sensitivity to initial weights is a general problem of neural networks (see for example, Kolen and Pollack, 1990, and Bezdek and Tsao, 1993). However, when 3rd order neurons were evaluated on the Iris data with random initial weights[1], they performed with *average* 5% misclassifications. Thus, the capacity of neurons to be 'spread' over volumes may provide new possibilities for addressing the initialization problem.

- **Computational cost**. The need to invert a high order tensor introduces a significant computational cost, especially when the input dimensionality is large. There are some factors that counterbalance this computational cost: (a)

the covariance tensor needs to be inverted only when a neuron is updated, not when it is activated or evaluated. When the neuron is updated, the inverted tensor is computed and then stored and used whenever the neuron needs to compete or evaluate an input signal. This means the whole layer will need only one inversion for each training point and no inversions for non-training operation. (b) Because of the complexity of each neuron, sometimes less of them are required. (c) Relatively complex shapes can be attained with low orders (say, 3rd order).

- **Selection of neuron order.** As in many other networks, there is much domain knowledge about the problem that comes into the solution through choice of parameters such as the *order* of the neurons. However, we also estimate that due to the rather analytic representation of each neuron, and since high order information is contained with each neuron independently, this information can be directly extracted (using the eigentensors). Thus, it is relatively easy to analytically decompose a cross-shapes 4th order cluster into two overlapping elliptic clusters, and vise versa.

- **Stability vs. flexibility and enforcement of particular shapes.** Further research is required to find methods for biasing neurons towards particular shapes, in attempt to seek particular shapes and to help neuron stability. For example, how would one encourage detection of triangles and not rectangles?

- **Non polynomial base functions.** We intend to investigate the properties of shape layers based on non-polynomial base functions. Noting that the high-order homogeneous tensors give rise to various degrees of polynoms, it is possible to derive such tensors with other base functions such as wavelets, trigonometric functions and other well-established kernel functions. Such an approach may enable modeling arbitrary geometrical shapes.

7 Acknowledgements

We thank Eitan Domani for his helpful comments and insight. This work was supported in part by the U.S.-Israel Binational Science Foundation (BSF), by the Israeli ministry of arts and sciences, and by the Fund for Promotion of Research at the Technion. Hod Lipson acknowledges the generous support of the Charles Clore Foundation and the Fischbach Postdoctoral Fellowship.

Download further information, MATLAB demos and implementation details of this work from *http://www.cs.brandeis.edu/~lipson/papers/geom.htm*

8 References

Abe S., Thawonmas R., 1997, "A fuzzy classifier with ellipsoidal regions", *IEEE Trans. On Fuzzy Systems*, Vol. 5, No. 3, pp. 358-368

Anderson E., "The Irises of the Gaspe Peninsula," Bulletin of the American IRIS Society, Vol. 59, pp2-5, 1939.

Balestrino A., Verona B. F., 1994, "New adaptive polynomial neural network", *Mathematics and Computers in Simulation*, Vol. 37, pp. 189-194

Bishop, C. M., 1997, *Neural Networks for Pattern Recognition*, Clarendon press, Oxford

Blatt, M., Wiseman, S. and Domany, E., 1996, "Superparamagnetic clustering of data", *Physical Review Letters*, 76/18, pp. 3251-3254

Davé R. N., 1989, "Use of the adaptive fuzzy clustering algorithm to detect lines in digital images", in *Proc. SPIE, Conf. Intell. Robots and Computer Vision*, SPIE Vol. 1192, No. 2, pp. 600-611

Duda R. O., and Hart, P. E., 1973, *Pattern classification and scene analysis*, New York, Wiley.

Faux I. D., Pratt M. J., 1981, *Computational Geometry for Design and Manufacture*, John Wiley & Sons, Chichester

Frigui, H. and Krishnapuram, R., 1996, "A comparison of fuzzy shell-clustering methods for the detection of ellipses", *IEEE Transactions on Fuzzy Systems*, 4/2, pp. 193-199

Giles C. L., Griffin R. D., Maxwell T., 1988, "Encoding geometric invariances into higher-order neural networks", in Anderson D. Z. (Ed.), *Neural Information Processing Systems*, American Institute of Physics Conference Proceedings

Gnanadesikan, R., 1977, *Methods for statistical data analysis of multivariate observations*, Wiley, New York

Goudreau M. W., Giles C. L., Chakradhar S. T., Chen D., 1994, "First-order versus second-order single layer recurrent neural networks", *IEEE Transactions on Neural Networks*, Vol. 5, No. 3, pp. 511-513

Graham A., 1981, *Kronecker products and Matrix Calculus: with Applications*, Wiley, Chichester

Gustafson E. E. and Kessel W. C., 1979, "Fuzzy clustering with fuzzy covariance matrix", in *Proc. IEEE CDC*, San Diego, CA, pp. 761-766

Haykin, S., 1994, *Neural Networks, A comprehensive foundation*, Prentice Hall, New Jersey

Kavuri, S.N. and Venkatasubramanian, V., 1993,

"Using fuzzy clustering with ellipsoidal units in neural networks for robust fault classification", *Computers Chem. Eng.*, 17/8, pp. 765-784

Kohonen, T., 1997,"Self organizing maps", Springer Verlag, Berlin

Kolen J. F., Pollack J. B., 1990, "Back propagation is sensitive to initial conditions", *Complex systems*, Vol. 4 No. 3, pp. 269-280

Krishnapuram, R., Frigui, H. and Nasraoui, O., 1995, "Fuzzy and possibilistic shell clustering algorithms and their application to boundary detection and surface approximation - Parts I and II", *IEEE Transactions on Fuzzy Systems*, 3/1, pp. 29-60.

Lipson, H., Hod, Y. and Siegelmann, H. T., 1998, "High-Order Clustering Metrics for Competitive Learning Neural Networks", to appear, *Proceedings of the Israel-Korea Bi-National Conference on New Themes in Computer Aided Geometric Modeling*, Tel-Aviv, Israel, Feb 18-19.

Mao, J. and Jain, A., 1996, "A self-organizing network for hyperellipsoidal clustering (HEC), *IEEE Transactions on Neural Networks*, 7/1, pp. 16-29.

Mclachlan G. J., Krishnan T., 1997, *The EM algorithm and extensions*, Wiley-interscience, New york

Myung I., Levy J., William B., 1992, "Are higher order statistics better for maximum entropy prediction in neural networks?", *Proceedings of the Int. joint conference on neural networks IJCNN'91*, Seattle WA., p. 967

Pal, N., Bezdek, J.C. and Tsao, E.C.-K., 1993, "Generalized clustering networks and Kohonen's self-organizing scheme", *IEEE Transactions on Neural Networks*, 4/4, pp. 549-557

Pan, J.S., McInnes, F.R. and Jack, M.A., 1996, "Fast clustering algorithms for vector quantization" *Pattern Recognition*, 29:3, pp. 511-518.

Pollack J. B., 1991, "The induction of dynamical recognizers", *Machine Learning*, Vol. 7, pp. 227-252

Schrock E., duManoir S., Veldman T., Schoell B., Wienberg J., Feguson Smith M. A., Ning Y., Ledbetter D. H., BarAm I., Soenksen D., Garini Y., Ried T, 1996, "Multicolor spectral karyotyping of human chromosomes", *Science*, Vol. 273, No. 5274, pp. 494-497